

# Fast Active Power-Frequency Support Methods by Large Scale Electrolyzers for Multi-Energy Systems

Nidarshan Veerakumar, Zameer Ahmad  
Intelligent Electrical Power Grids  
Delft University of Technology  
Delft, Netherlands  
[N.K.VeeraKumar@tudelft.nl](mailto:N.K.VeeraKumar@tudelft.nl)

M. Ebrahim Adabi  
Intelligent Electrical Power Grids  
Delft University of Technology  
Delft, Netherlands  
[ebrahim.adabi@tudelft.nl](mailto:ebrahim.adabi@tudelft.nl)

José Rueda Torres  
Intelligent Electrical Power Grids  
Delft University of Technology  
Delft, Netherlands  
[j.l.ruedatorres@tudelft.nl](mailto:j.l.ruedatorres@tudelft.nl)

Peter Palensky  
Intelligent Electrical Power Grids  
Delft University of Technology  
Delft, Netherlands  
[P.Palensky@tudelft.nl](mailto:P.Palensky@tudelft.nl)

Mart van der Meijden  
TenneT TSO B.V.  
Delft University of Technology  
Delft, Netherlands  
[Mart.vander.Meijden@tennet.eu](mailto:Mart.vander.Meijden@tennet.eu)

Francisco Gonzalez-Longatt  
Institutt for elektro, IT og kybernetikk  
Universitetet I Sørøst-Norge  
Porsgrunn, Norway  
[f.longatt@fglongatt.org](mailto:f.longatt@fglongatt.org)

**Abstract**— This paper presents a comparative assessment of fast active power regulation (FAPR) control strategies implemented on megawatt-scale controllable electrolyzers, with the goal of achieving enhanced frequency support during large active power imbalances that lead to major under-frequency deviations. The FAPR control strategies consist of three different types of controllers, namely, droop, derivative and Virtual Synchronous Power (VSP). Each of these controllers has been implemented on a 300 MW electrolyser plant with proton exchange membrane (PEM) electrolyzers. The compared FAPR controllers are individually set to perform a fast adjustment of the active power consumption of the plant-based on the dynamic grid conditions. The modelling and comparative assessment is done in a platform for computationally efficient simulations of Electromagnetic Transients (EMT) in real-time. A synthetic model of the Northern Netherlands Network (N3 Network) is prototyped as a test bench to simulate and evaluate the performance of the implemented FAPR controllers. The EMT simulations show the superiority of the VSP based FAPR developed for controlling and exploiting the boundaries for active power adjustment of the Voltage Source Converter (VSC) that interfaces the PEM electrolyser plant with the N3 Network.

**Keywords**— Frequency Droop and Derivative Controller, VSP Controller, Inertia emulation, RTDS, PEM Electrolyser.

## I. INTRODUCTION

The common definition of frequency stability depicts that it is the ability of a power system to safeguard the time evolution of the system frequency within acceptable technical limits, after the occurrence of a disturbance that alters the overall active power balance [1]-[3]. Once the active power balance is altered, the inherent inertial response of the rotating masses in operation, and the primary frequency control systems distributed across the power system are expected to kick-in and arrest the imbalance, thereby attempting to mitigate the rate-of-change-of-frequency (RoCoF) and to limit the maximum frequency excursion from the pre-disturbance (steady-state) frequency value. Ensuring the effectiveness of the overall inertial response and the primary frequency control of multi-energy systems constitutes a significant challenge due to the phase-out of conventional, especially fossil fuel-fired power plants, with synchronous generators. In this context, advanced controllers for fast active power-frequency control are needed to quickly and effectively adjust the active power at the AC side of the power electronic converters (e.g. Voltage Source Converters) used to interface renewable energy-based generation systems and responsive loads (e.g. electrolyzers).

While significant research effort is being devoted to the fast active power frequency control for renewable energy-based generation, the focus of this paper is on the deployment of multi-megawatt scale electrolyser plants to support the frequency stability multi-energy systems. To facilitate this function, a supplementary control loop attached to the outer control loops of the VSC interface of the electrolyser is proposed for fast regulation of the active power consumption of the electrolyzers. The study presented in this paper takes into account the situation of under-frequency events, which should be mitigated through the electrolyser's FAPR controller. For illustrative purposes, an under frequency event, which can be caused by a sudden generation outage or a sudden increase in load, is depicted in Figure 1. Note in the figure, that FAPR is expected to significantly improve the dynamic frequency response by promptly and effectively bounding the RoCoF and the frequency Nadir.

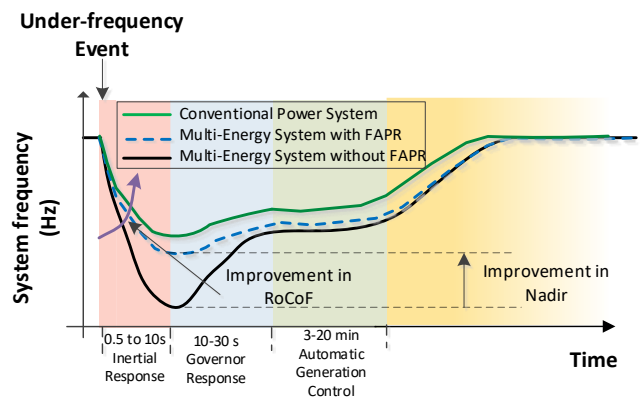


Figure 1. Expected influence of FAPR in under-frequency events.

As illustrated in Figure 1, the time frame of operation of FAPR may ideally overlap with the typical time frame of the inertial response of generators (e.g. 500ms from the disturbance of active power). Different forms of FAPR, ranging from proportional (droop) based control [4]-[7], emulation of inertia of synchronous generators [8]-[10], to several types of de-loading techniques [11] have been investigated in the last 10 years. However, all of these studies are confined to applications in renewable power generation [12].

Although some studies have been conducted to address the feasibility of using proportional control in small-size (kW scale) loads [13]-[17], there is no insight on the feasibility and degree of enhancement of frequency stability that can be

brought by performing FAPR in large-size (multi-megawatt scale) responsive loads. This paper bridges this gap in the current state-of-the-art by developing and comparing the performance of three different forms of FAPR for a 300 MW PEM electrolyser plant. The first form is the traditional proportional (droop) based approach, the second one follows the principles of the derivative controller, whereas the third one is a simplified (second-order) variant of the virtual synchronous power (VSP) that is currently being investigated in applications concerning with renewable power generation.

The detailed modelling and comparative assessment is done in a platform for computationally efficient simulations of Electromagnetic Transients (EMT) in real-time. A synthetic model of the Northern Netherlands Network (N3) is prototyped as a test bench to simulate and evaluate the performance of the FAPR controllers attached to the 300 MW PEM electrolyser.

The subsequent sections of this paper are organised as follows: In Section II, the PEM electrolyser model and its control structure are explained. In section III, the developed forms of FAPR are presented. Section IV presents the comparative study performed by using the N3 network with generation and demand scenarios projected for the year 2030. A summary of concluding remarks is given in Section V.

## II. MODELLED FUNCTIONS OF PEM ELECTROLYSER

In electrolyzers, the electrochemical process of water electrolysis is performed: the water is divided into hydrogen and oxygen by controlling DC power supply. Anion Exchange Membrane (AEM), Solid Oxide Electrolyzers (SOE) electrolyzers, alkaline electrolyzers, and PEM electrolyzers are the main four types of electrolyser [12]. The two main electrolyser technologies that are undergoing developments towards large-scale (e.g. multi-megawatt up to gigawatt) electrolysis facilities are alkaline and PEM electrolyzers [18]-[22]. PEM electrolyser provides benefits such as lower financial expenses and more efficient dynamic performance. Hence, PEM electrolyser technology is chosen for this study.

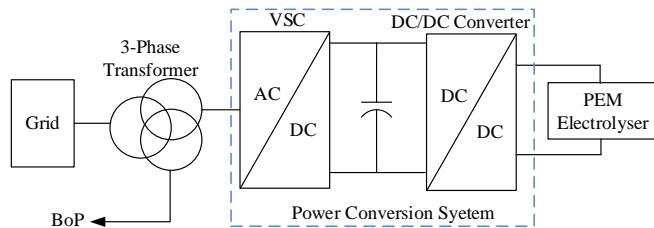


Figure 2. Interfacing Power electronic components between Grid and PEM Electrolyser

Figure 2 shows the electrical connection of a PEM electrolyser, as it is modelled in this study. As it can be observed from the figure, the electrolyser needs a DC power supply, which is provided through the grid-connected three-phase AC/DC converter linked in series with a DC/DC converter. The balance of plant (BoP) components are represented by a constant load since it can be assumed that they have a fixed power consumption [23].

Figure 3 shows the overall schematic for the outer control system of the PEM electrolyser as defined in [24]-[26]. The schematic contains three functions: FAPR control for frequency tracking, voltage tracking, and active/reactive control. Also, it should be noted that such a system is open to extensions (to be done in future works) to have the capability to communicate and respond simultaneously to the signals sent, for instance, from market, transmission system operators, and local alarms. The output signals ( $i_{dref}$ ,  $i_{qref}$ ) from the outer control system will serve as the reference signal for inner current controllers. Figure 4, shows the inner current controllers designed for the VSC, shown in Figure 2. A vector oriented control (VOC) strategy has been selected to generate proper reference signals for the PWM modulation technique for VSC [27]-[28].

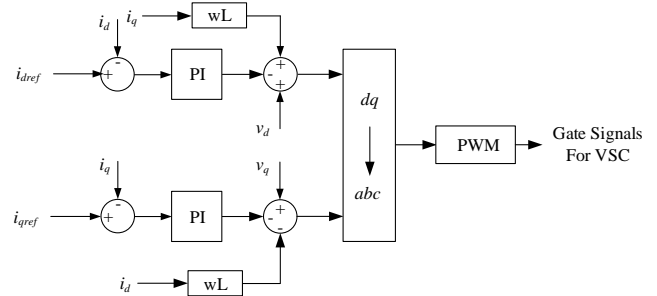


Figure 4. Inner controller structure of PEM electrolyser

## III. FAPR CONTROLLERS

Three different forms of FAPR control can be added into the FAPR block shown in Figure 3. The rationale behind each of these forms is described in the following subsection.

### A. Droop based FAPR controller

Figure 5 shows the control block diagram of the droop based FAPR controller. The frequency ( $f$ ) is measured in the synthetic N3 network using phasor measurement units (PMU) as shown in Figure 3. The measured frequency is compared with the reference frequency which is 50Hz for the N3 Network; the frequency error is then passed through a deadband for selective operation of the controller. The deadband is a system-dependent component which should be fixed based on the behaviour of frequency under an under-frequency event to avoid unnecessary activation of FAPR controllers [29].

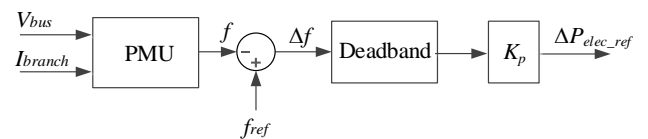


Figure 5. Droop based FAPR controller.

Further, this frequency error signal ( $\Delta f$ ) is amplified using a proportional gain ( $K_p$ ), and will determine the amount of active power reduction signal ( $\Delta P_{elec\_ref}$ ) to support system frequency. As shown in Figure 3, the output of FAPR controller,  $\Delta P_{elec\_ref}$ , is added as an auxiliary reference signal which activates only during load imbalance event to determine the reference signal for the active power of electrolyser.

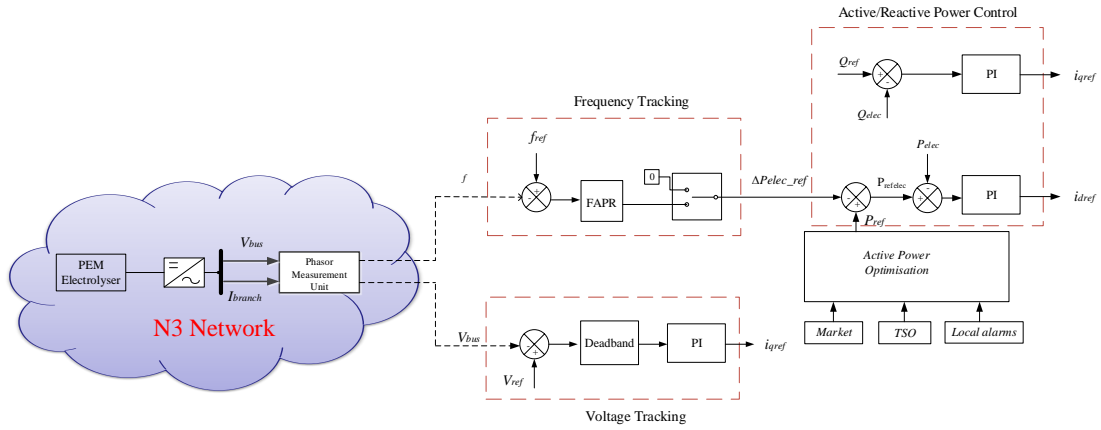


Figure 3. Outer controller structure of PEM electrolyser

### B. Combined Droop-Derivative based FAPR controller

Derivative-based FAPR control approach is where the active power is regulated due to frequency deviation with respect to reference/nominal frequency under the condition of dynamically changing generations/loads. Figure 6, demonstrates the combined droop and derivative-based FAPR controller for electrolyser. In this controller, as the name suggests is a combination of two controllers, namely droop controller and derivative controller.

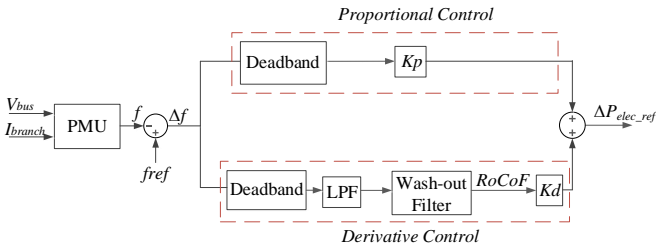


Figure 6. Combined droop and derivative-based FAPR

Combined droop and derivative-based FAPR, provides higher ramped signal values which is required for the initial arrest of frequency change during the containment period after the occurrence of under-frequency event. As seen from Figure 6, the derivative term has been realized through the combination of low pass filter (LPF) and Wash-out filter. The parameters for the low-pass and the washout filter are selected in a way that to achieve a proper response at the output of the derivative block. Moreover, the derivative term is multiplied with a value called derivative gain ( $K_d$ ) to tune the effect of the derivative block. Finally, the signal achieved through derivative control and droop control will be combined to form the output signal of FAPR controller  $\Delta P_{elec\_ref}$ .

### C. VSP based FAPR Controller

Figure 7 shows the control diagram for the virtual synchronous power (VSP) controller. Unlike other forms (high order non-linear functions with multiple parameters to be tuned) of VSP proposed in existing literature for renewable power generation or HVDC links, and as it can be observed from this figure, VSP has a second-order transfer function. This function enables simultaneous control of damping and overshoot into the system. This is possible when tuning  $\omega_n$  (to influence the natural frequency of electromechanical oscillations) and  $\zeta$  (the damping factor). With the help of VSP based controller, the dynamics of frequency response has improved in comparison with the droop and combined droop and derivative methods. The frequency measurement which

is achieved through PMU will be compared with the reference frequency of 50Hz and the frequency error, if it falls outside the deadband is injected as an input to the 2<sup>nd</sup> order function block. The 2<sup>nd</sup> order transfer function is tuned in such a way to have a desired rise time and amplitude. The resulting signal from VSP based FAPR controller forms,  $\Delta P_{elec\_ref}$ , which further sets the active power reference required for the PEM Electrolyser.

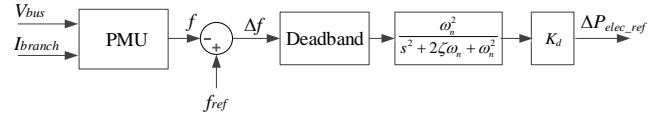


Figure 7. VSP based FAPR controller

## IV. SIMULATION RESULTS

### A. Test case description

A synthetic EMT model of the North of Netherlands system has been implemented in a real-time digital simulator, by using the functions of the RSCAD software, developed for version 5.006.1. Compared to tools typically used for off-line EMT simulations (e.g. PSCAD), RTDS is preferred for this analysis since it is significantly more computationally efficient (e.g. 1 s of EMT simulation does not take several minutes) and also allows in future to interface a software (RSCAD) based model with an actual hardware to perform controller testing in a near-real practice context. The layout of the system is shown in Figure 8. Based on [30], a scenario for the year 2030 was projected. The total assumed generation is 3490 MW. To study the contribution of electrolysers to frequency stability, the FAPR controllers are tested against an under frequency event. It corresponds with a 200MW sudden and stepwise decrease of the total output power of the Gemini wind power plant.

### B. Results Description

The 300 MW PEM Electrolyser model present in the synthetic model of the N3 system has been modified to react with either droop, combined droop-derivative, or VSP based FAPR controller. During the under-frequency event, caused by a sudden loss of 200 MW decrease of the output power of the Gemini wind power plant, the PEM electrolyser should rapidly reduce its active power absorption to mitigate the frequency deviation. Figure 9 shows the instantaneous variation of the active power response of the PEM electrolyser, which is in line with the active power reference. Figure 10 depicts the frequency response related to three

different mentioned FAPR controllers. As observed in Figure 9 and Figure 10, red line representing a base case, where there is no provision of frequency support from the electrolyser. Therefore, the consumed active power of the electrolyser remains constantly unchanged as 300 MW. Hence it can be seen from the frequency curve, a value of 49.815 Hz has been achieved, so with FAPR controllers, the task is to increase the Nadir value along with decreasing rate of change of frequency (RoCoF).

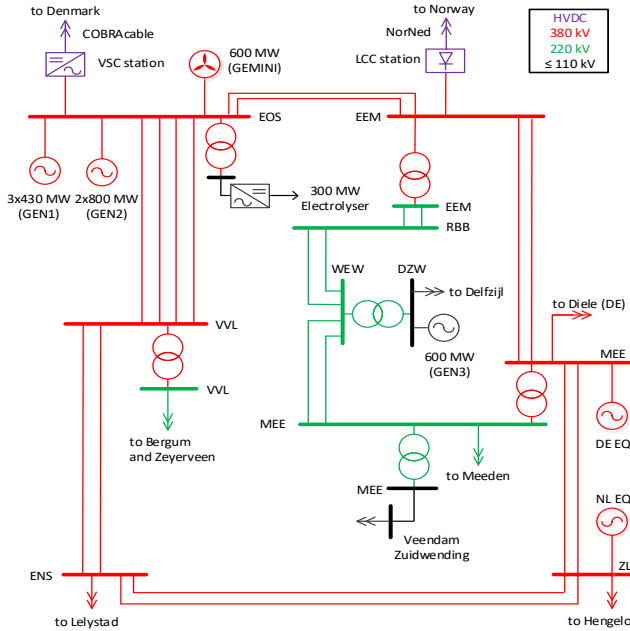


Figure 8. North of Netherlands Network for the year 2030

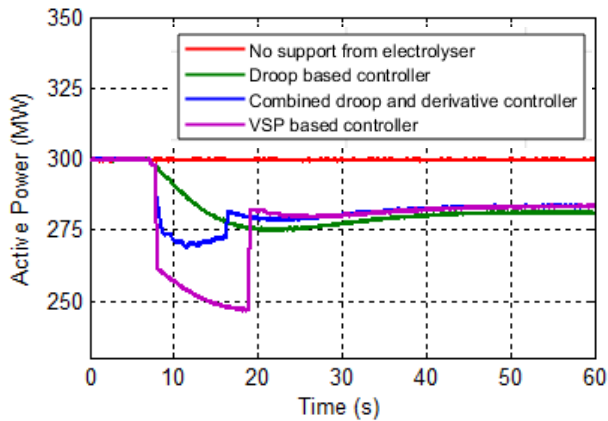


Figure 9. Power Response from electrolyser due to FAPR controllers

With operational droop based FAPR controller, based on the continuous sensing of the frequency deviation, the active power demand of the PEM electrolyser was reduced, resulting in an increase of frequency nadir value as seen from the green line. With the combined droop-derivative FAPR controller in action, along with an improvement in frequency Nadir, a better RoCoF response can be achieved as observed from the blue line of Figure 10. This is due to a faster active power reduction through a derivative action added in parallel to the droop function.

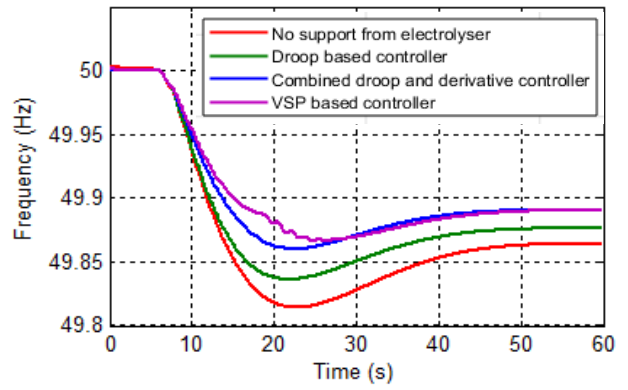


Figure 10. Frequency Response from electrolyser due to FAPR controllers

Also, due to the derivative action, there is an improvement in the de-ramp of the rate of the frequency deviation. Since this signal multiplied with a derivative gain  $K_d$ , provides enough de-ramp rate for the electrolyser for quick initial active power decay. With VSP based FAPR controller, as seen from the red line in Figure 10, greater improvement has been achieved for both RoCoF and Nadir. This is possible due to the second order transfer function block, where it is possible to better tune the rise time avoiding undamped oscillation. As seen from Figure 9, for combined droop and derivative-based controller, initial decay of 26 MW has been achieved with a slight compromise with low-frequency oscillations. However, for the VSP based controller, initial decay up to 40 MW can be easily achieved. Also, it is noteworthy that once the derivative or the VSP controller action is deactivated (after 10.0 s – the deactivation time shall be tuned in each system depending on the inherent dynamic behaviour), the active power reference shifts back to droop function, this non-smooth shift in the controller will have undesirable ripple effects on the frequency curve as seen from the purple line in Figure 10. The study performed in this work constraints to under-frequency phenomenon, this work cannot be extended to over-frequency due to physical limitations of electrolyser, unless operated lower than rated condition. Also, in general FAPR should be tuned such that the maximum allowed reduction in active power should not fall below 30% of the rated value, owing to the characteristic curve of PEM electrolyser[12],[24].

## V. CONCLUSIONS

This paper presents and provides a comparative assessment of the performance of three different forms of FAPR that can be applied to multi-MW scale electrolysis plants. The goal is to understand the feasibility of these control functions and their effectiveness when supporting the primary frequency control in a multi-energy system. The first form is the traditional proportional (droop) based approach, the second one follows the principles of the derivative controller, whereas the third one is a simplified (second-order) variant of the VSP. The study is conducted by using the synthetic model of the Northern Netherlands Network, by considering a projected scenario of generation-demand by the year 2030, as well as by taking into account the presence of a 300 MW PEM electrolyser plant.

The simulation results achieved through EMT simulations show the superiority of VSP based FAPR controller, which

can provide more efficient improvement in both frequency Nadir and RoCoF. Since VSP based FAPR offers two parameters to tune its dynamic response, it has been observed via EMT simulations, that it entails a smaller overshoot and damping factor, when compared against the response of the combined droop and derivative FAPR controller. This leads to a safe fast adjustment of the consumed active power by the megawatt-scale PEM electrolyser, thereby promptly and effectively contributing to bound the dynamic frequency response in within initial seconds after the occurrence of an active power imbalance. The EMT simulations also showed that no extra design requirements (e.g. temporary overload) would be needed for the VSC used in the PEM electrolyser. It was also observed that the DC voltage of the VSC remains within acceptable bounds when using any of the implemented FAPR controllers.

#### ACKNOWLEDGEMENT

This work has received funding from the European Union's Connecting Europe Facility (CEF) programme under the grant agreement No INEA/CEF/SYN/A2016/1336043 – TSO2020 Project (Electric “Transmission and Storage Options” along TEN-E and TEN-T corridors for 2020). This paper reflects only the authors' views, and the European Commission is not responsible for any use that may be made of the information it contains.



**Co-Financed by the European Union**  
Connecting Europe Facility

#### REFERENCES

- [1] P. Kundur et al., “Definition and Classification of Power System Stability,” *IEEE Trans. Power Syst.*, vol. 19, no. 3, pp. 1387–1401, 2004.
- [2] P. Tielens and D. Van Hertem, “The relevance of inertia in power systems,” *Renew. Sustain. Energy Rev.*, vol. 55, no. 2016, pp. 999–1009, 2020.
- [3] E. Rakhshani, J. Sadeh, “Practical Viewpoints on Load Frequency Control Problem in a Deregulated Power System”, *Energy conversion and management*, Vol. 51. Issue 6. pp. 1148-1156. June 2010.
- [4] S. Mishra, P. Zarina, P. Sekhar, “A novel controller for frequency regulation in a hybrid system with high PV penetration,” In: *IEEE Power and Energy Soc General Meeting (PES)*, p. 1–5, 2013.
- [5] F. Gonzalez-Longatt, E. Chikuni, E. Rashayi, “Effects of the synthetic inertia from wind power on the total system inertia after a frequency disturbance,” *Proceedings of IEEE Ind Technol Conference*, 2013.
- [6] E. Jahan, M. d. Rifat Hazari, et. al, “ Primary frequency regulation of the hybrid power system by deloaded PMSG-based offshore wind farm using centralised droop controller,” *The Journal of Engineering*, vol. 2019, Issue.18, pp. 4950-4954, 2019.
- [7] R. Josephine, S. Suja, “Estimating PMSG wind turbines by inertia and droop control schemes with intelligent fuzzy controller in Indian,” *Dev J Elect Eng Technol*, vol. 9, pp. 1196–201, 2014.
- [8] E. Rakhshani, P. R. Cortes, “Inertia Emulation in AC/DC Power Systems Using Derivative Technique Considering Frequency Measurement Effects”, *IEEE Transactions on Power Systems*, Volume: 32, Issue: 5, 2017.
- [9] R. Eriksson, N. Modig, and K. Elkington, “Synthetic inertia versus fast frequency response : a definition,” *IET Renew. Power Gener.*, vol. 12, no. 5, pp. 507–514, 2018.
- [10] M. Dreidy, H. Mokhlis, and S. Mekhilef, “Inertia response and frequency control techniques for renewable energy sources: A review,” *Renew. Sustain. Energy Rev.*, vol. 69, no. July 2016, pp. 144–155, 2017.
- [11] M. H. Syed, E. Guillo-Sansano, et. al., “Enhanced load frequency control: incorporating locational information for temporal enhancement,” *IET Gener. Transm. Distrib.*, vol. 13, no.10, pp. 1865–1874, 2019.
- [12] P. K. S. Ayivor, “ Feasibility of Demand Side Response from Electrolysers to support Power System Stability,” MSc. thesis, Delft University of Technology, Delft, the Netherlands, 2018.
- [13] J. Eichmann, K. Harrison and M. Peters, “Novel Electrolyser Applications: Providing More Than Just Hydrogen,” Technical Report NREL/TP-5400-61758, National Renewable Energy Laboratory, Denver CO, USA, September 2014.
- [14] V. Ruuskanen, J. Koponen, K. Huoman, A. Kosonen, M. Niemelä, and Ahola, “PEM water electrolyzer model for a power-hardware-in-loop simulator,” *International Journal of Hydrogen Energy*, vol. 42, no.16, pp.10775-10784, 2017.
- [15] Xu, H., Kockar, I., Schnittger, S., Rose, J.: ‘Influences of a hydrogen electrolyser demand on distribution network under different operational constraints and electricity pricing scenarios’, *CIREC Workshop*, Helsinki, Finland, June 2016.
- [16] Alrewq, M., Albarbar, A.: ‘Investigation into the characteristics of proton exchange membrane fuel cell-based power system’, *IET Science, Measurement & Technology*, vol. 10, no. 3, pp. 200–206, 2016.
- [17] H.-i. Kim, C. Y. Cho, J. H. Nam, D. Shin, and T.-Y. Chung, “A simple dynamic model for polymer electrolyte membrane fuel cell (PEMFC) power modules: Parameter estimation and model prediction,” *International journal of hydrogen energy*, vol. 35, no. 8, pp. 3656–3663, Apr. 2010.
- [18] P. Ayivor, J. Torres, M.A.M.M. van der Meijden, R. van der Pluijm, and B. Stouwie, “Modelling of Large Size Electrolyzer for Electrical Grid Stability Studies in Real Time Digital Simulation,” in *Proc. of Energynautics 3rd International Hybrid Power Systems Workshop*, Tenerife, Spain, May 2018.
- [19] P. Ayivor, J.L. Rueda Torres, and M.A.M.M. van der Meijden, “Modelling of Large Size Electrolyser for Electrical Grid Stability Studies - A Hierarchical Control,” in *Proc. 17th Wind Integration Workshop*, Stockholm, Sweden, October 2018.
- [20] R. Harvey, R. Abouatallah, and J. Cargnelli, “Large-scale water electrolysis for power-to-gas,” in *PEM Electrolysis for Hydrogen Production: Principles and Applications*, 2016, pp. 303-313.
- [21] K. Agbli, M. Péra, D. Hissel, O. Rallières, C. Turpin, and I. Dombia, “Multiphysics simulation of a PEM electrolyser: Energetic macroscopic representation approach,” *International journal of hydrogen energy*, Vol. 36, No.2, 2011.
- [22] M. Lebbal and S. Lecoeuche, “Identification and monitoring of a PEM electrolyser based on dynamical modelling,” *International journal of hydrogen energy*, Vol. 34, No. 14, 2009.
- [23] H. Vogelesang, “An introduction to energy consumption in pumps,” *World pumps*, Vol. 2008, No. 496, 2008.
- [24] V. Suárez, P. Ayivor, J. Torres, and M.A.M.M. van der Meijden, “Demand side response in multi-energy sustainable systems to support power system stability,” presented at 16th Wind Integration Workshop, Berlin, Germany, 2017.
- [25] F. Alshehri, V. García and J.L. Rueda, A. Perilla and M.A.M.M. van der Meijden, “Modelling and evaluation of PEM hydrogen technologies for frequency ancillary services in future multi-energy sustainable power systems” *Elsevier Heliyon*, Vol. 5, no. 4, 2019.
- [26] S. Leng, “ Coordination of multiple active front end converters for power quality improvement,” Ph.D. thesis, The Florida State University, 2012.
- [27] A. Yazdani and R. Iravani, “A unified dynamic model and control for the voltage-sourced converter under unbalanced grid conditions,” *IEEE Trans. on Power Del.*, vol. 21, no.3, pp. 1620–1629, July 2006.
- [28] L. Xu, B. Andersen, and P. Cartwright, “VSC transmission operating under unbalanced AC conditions-Analysis and control design,” *IEEE Trans. on Power Del.*, vol. 20, pp. 427–434, Jan. 2005.
- [29] Migrate Work Package 1, MIGRATE Deliverable D1.6: Power system risk analysis and mitigation measures, (2019).
- [30] “Stability Analysis of an International Electricity System connected to Regional and Local Sustainable Gas Systems”, *TSO 2020 Activity 2 Final Report*, 2019.